IEEE Access
Multidisciplinary ⋮ Rapid Review ⋮ Open Access Journal

Received 1 March 2023, accepted 10 March 2023, date of publication 15 March 2023, date of current version 21 March 2023.

Digital Object Identifier 10.1109/ACCESS.2023.3257414

RESEARCH ARTICLE

A Study of Drift Effect in a Popular Metal Oxide Sensor and Gas Recognition Using Public Gas Datasets

IL-SIK CHANG[1], SUNG-WOO BYUN[2], TAE-BEOM LIM[2], (Member, IEEE), AND GOO-MAN PARK[3]

[1]Graduate School of Nano IT Design Fusion, Seoul National University of Science and Technology, Seoul 01811, South Korea
[2]Korea Electronics Technology Institute, Jeonju 13509, South Korea
[3]Department of Information Technology and Media Engineering, Seoul National University of Science and Technology, Seoul 01811, South Korea

Corresponding author: Goo-Man Park (gmpark@seoultech.ac.kr)

This work was supported by the Institute of Information and Communications Technology Planning and Evaluation (IITP) Grant funded by the Korean Government through Ministry of Science and ICT (Intelligent e-nose development for gas detection to sub-ppb level) under Grant 2020-0-01106.

ABSTRACT Metal oxide sensor is widely used in many research fields, including E-nose for gas detection due to their tunable sensitivity, space efficiency and low cost. One of the most popular open data sets in electronic nose research contains data on various gases sampled using a MOx sensor in a wind tunnel over 16 months. A recent study published in 2022 by Nik Dennler has reported the discovery of the drift effect of a public dataset due to incorrect experimental design. they reported that the order of gas collection was not randomized and further discovered that a select set of gases were collected over a particular period. This paper expands the previous paper, by analyzing the drift effect with low signal, zero-offset subtracted signal's mean, and standard deviation value by location and time, and examining it with TSNE, a dimensional reduction method. In addition, the accuracy by time and location was analyzed by applying it to various Deep Learning methods. According to the results, we confirmed that gas information is already classified before the gas leaks in terms of temporal and spatial domain. Therefore, the classification accuracy overestimates the actual accuracy that can be obtained due to the drift effect. Based on the results of this study, it is necessary to thoroughly verify the temporal and spatial validity of the gas dataset when using the publicly available gas dataset to develop gas detection algorithms.

INDEX TERMS Metal oxide sensor, drift effect, gas recognition, electronic nose system, artificial olfactory.

I. INTRODUCTION

Over the past 50 years, the research field of electronic noses has developed rapidly with the growth of information technology [1]. The critical goal of artificial olfactory research is to classify various materials with high specificity; this requires multiple gas sensor arrays with relatively high selectivity and low specificity alongside a pattern recognition algorithm to predict what materials are exposed. Since Taguchi commercialized a SnO2-based MOX (Metal OXide) gas sensor in 1968, MOX gas sensors have been widely used due to their various advantages (such as high sensitivity, low cost, long life, and succinct peripheral circuits). Mox sensors are excellent at detecting a wide range of gases and provide relative output depending on the variation of the gas density. Since Persaud and Dodd [2] first introduced the concept of imitating human olfactory senses using sensor arrays and pattern-recognition technology in 1982, Gardner and Bartlett [3] defined an electronic nose as a configuration of a sensor array that does not have complete selectivity for detecting odors or a pattern-recognition system that can differentiate simple odors from complex odors. Since then, MOX gas sensors have been adopted as a major sensor in electronic noses, and the low selectivity of MOX gas sensors has been improved dramatically by implementing pattern recognition technology using arrays. However, a crucial flaw of MOx sensors is their sensitivity to sensor drift (unpredictable alterations in the signal response upon continuous

The associate editor coordinating the review of this manuscript and approving it for publication was Aijun Yang.

exposure to uniform material) [4]. Sensor drift is primarily caused by chemical and physical interactions of a sensor site, such as sensor aging (restructuring of a sensor's surface over time) and sensor poisoning (irreversible or slowly reversible combinations of previously measured gases or other contaminants). Environmental factors such as changes in humidity, temperature, and pressure also affect sensor response. The effects of sensor drift can be reduced in the experiment planning process by assigning random materials to be exposed in the data-selection process. As another option, it is crucial to construct an analysis algorithm by remaining cognizant of the presence of sensor drifts.

One of the most popular open data sets in electronic nose research contains data on various gases sampled using a MOx sensor in a wind tunnel over 16 months [5]. This data set was utilized in gas classification algorithms, gas source location predictions, and other applications. Recent research has reported on the fundamental limitations of data sets; they reported that the order of gas collection was not randomized and further discovered that a select set of gases were collected over a particular period. Consequently, the sensor data had been corrupted by sensor drift [6].

This paper aims to analyze the effects of sensor drift on gas sensor data sets from temporal and spatial perspectives. For this, various experiments related to the drift effect are conducted using a data set from the MOx gas sensor array in a wind tunnel. First, the drift effect of sensor data over time and space is analyzed by measuring the change in sensor value before gas leaks. Second, learning gas classification model and recognizing eight gases to compare using the Zero-offset subtraction method for drift reduction vs. using raw signals. Lastly, the drift effect of gas data is analyzed by detecting gases using the OOD method since the electronic nose system should not be classified as a specific class until it has first been exposed to the gas.

The remainder of this paper is organized as follows: Section II presents the related works on electronic nose system. Section III and IV explain the public gas data analysis. Section V concludes this work.

II. RELATED WORKS

A. DATASET

Electronic devices and data analysis procedures must be specifically tailored to develop an electronic olfactory system. These designs and procedures must be created on reliable data. Public datasets are frequently used in the field of electronic olfactory research because they reduce the need for data collection during the early stages of the design of an electronic olfactory system [6]. Various datasets that include many different case studies, as well as tasks and applications, are publicly available [7], [8], [9]. Mox sensor data, collected from wind tunnels over 16 months for various experimental parameters and gases, is one of the most well-known datasets [5]. This data set contained 18,000 time-series data from ten different chemical gas substances, including acetone and acetaldehyde. It has also been incorporated into algorithms for identifying different types of gases, estimating the location of the gas source, and other applications. Vergara spent three years developing a dataset using an electronic nose system, which was made public in the UCI Machine Learning Repository [7]. This electronic nose system with 16 gas sensors collected six different types of gases, including ammonia.

B. ELECTRONIC NOSE SYSTEM

Even though the first studies on specific odor detection began in the 1920s, the idea of using chemical electronic sensor arrays to detect odors was primarily discussed, and [2] in the early 1980s. The term ''electronic nose'' appeared in [3] in the late 1990s to describe sensor arrays that could distinguish between one or more chemical components. With recent advancements in sensor technology, the application field has expanded significantly. Thanks to its dependable solutions, speed, affordability, and miniaturization, the e-nose is used in a variety of industries, including agriculture, food, medicine, and security [10], [11], [12], [13], [14].

Electronic nose systems with oxide semiconductor gas sensor arrays were thought to be promising platforms that could be improved to identify gases and odors using machine learning [15], [16], [17]. Due to their high sensitivity, quick response times, and simple structures, oxide semiconductor gas sensors have been widely used to detect harmful and toxic gases; however, the sensors' poor gas selectivity frequently limited their ability to detect these gases [18]. As a result, simple techniques such as PCA were used to analyze the sensing patterns obtained from the sensors [19], [20], and the performance of sensor arrays was subsequently improved using machine learning with various algorithms including artificial neural networks, convolution neural network (CNN), and recurrent neural networks (RNN) [21], [22], [23], [24].

C. DRIFT CORRECTION METHOD

Various approaches have been proposed in research to address the problem of drift, including drift compensation and drift correction. Drift correction can be broadly categorized into three approaches: 1) modeling methods that assume sensor drift can be modeled separately from the analysis signal, 2) composition correction methods that identify and remove components that are sensitive to drift before the model is built, and 3) adaptive correction methods based on machine learning. The first approaches frequently used baseline processing method and filtering method in frequency domain. These methods compensate for the response of each sensor. However, due to the complexity of the causes of drifting, these methods can only reduce some of the side effects caused by drift. The second approach attempts to identify and remove components sensitive to drifting before the model is constructed. However, since there is not enough prior information, these methods usually cannot effectively handle samples that differ significantly from the initial distribution. Adaptive correction methods were applied to drift revision through classifier integration by [25] for the first time in 2012. According to the experiment, an ensemble

method based on support vector machine was shown to deal well with sensor drifts and was certificated to fulfill the task better than baseline competing method. Domain adaptation and transfer learning approaches [26], [27], [28] focus on removing the influence of cross-domain sensitivity to make the prediction model more robust. The balanced distribution adaptor drift compensation method improved the accuracy of drift compensation by reducing the discrepancy between the two domains, as it can adjust the conditional and marginal distributions between the two domains through a weight balancing factor [25]. Additionally, to correct for drift and device variation, a transfer learning-based drift correction autoencoder model for adaptive domain adaptation was proposed [29].

III. GAS DATA ANALYSIS IN TERMS OF TIME AND SPACE

A. DATASET

The published gas sensor dataset comprises data collected from 18,000 time-series signals over 16 months by releasing 10 analysis gases (acetone, acetaldehyde, ammonia, butanol, methane, methanol, carbon monoxide, benzene, and toluene) [5]. The sensor platform consists of nine modules, each equipped with eight MOx sensors. They were placed at six different distances perpendicular to the wind direction from a gas inlet on a flat plate wind tunnel of size 2.5 m $\times$ 1.2 m $\times$ 0.4 m. Each sensor module was integrated with a sensor controller that enables data collection at a 100 Hz sampling speed and the airflow was adjusted by controlling the wind speed of the exhaust fan. Combinations of parameter gas, position, wind speed, and operating voltage were selected prior to measurement until each combination was repeated 20 times. This continued for 260 seconds and the gas was released from t = 20 seconds to t = 200 seconds. Data are saved in one file for each parameter combination.

B. GAS DATA ANALYSIS

The main task of the artificial olfactory sense is to identify different gas materials at high specificity. MOx sensors are mainly used for sensor arrays because they can streamline the layout, reduce costs, and save space. One critical demerit of a MOx sensor is that it has susceptibility to sensor drift. Drift occurs due to influences such as sensor deterioration and changes in temperature, humidity, or pressure. To reduce the influence of gas and sensor drift, the order of gas exhaust is assigned randomly. This paper analyzes drift's influences on the published gas datasets in terms of time and space.

The recording time was extracted from the file name to analyze the temporal sequence of gases. Table 1 shows that gas was collected in a specific sequence rather than in random order. Hence, it is assumed that the collected gas data were significantly influenced by the drift effect.

Figure 1 shows the sensor value in the 0–10 second section of the no. 5 Board at the L2 position, strongly influenced by gas, and the no. 9 Board at the L1 position, least affected by gas in chronological order. According to the results, values are distributed around 400 for all sensors on no. 9 Board at the L2 position that was less influenced by drift, and it is assumed that this is because the drift effect did not occur as it was less affected by the gas. In contrast, the sensor values are categorized by class even before the gas was released since the no. 5 Board at the L2 position was strongly influenced by gas. This could engender fatal errors in utilizing the e-nose system, so researchers are required to consider the drift effect before devising gas detectors. However, numerous previous types of research that used this dataset as one of the most popular datasets reported wrong results without considering the drift effect.

TABLE 1. The published gas sensor data sorted by time.

Day	Gas	Location
2010-12-07 23:02	CO	L6
2010-12-07 23:08	CO	L6
2010-12-07 23:14	CO	L6
2010-12-07 23:21	CO	L6
…	…	…
2011-06-02 17:15	Ammonia	L3
2011-06-02 17:21	Ammonia	L3
2011-06-02 17:28	Ammonia	L3
2011-06-02 17:34	Ammonia	L3
…	…	…
2011-07-21 18:19	Acetone	L3
2011-07-21 18:25	Acetone	L3
2011-07-21 18:31	Acetone	L3
2011-07-21 18:38	Acetone	L3

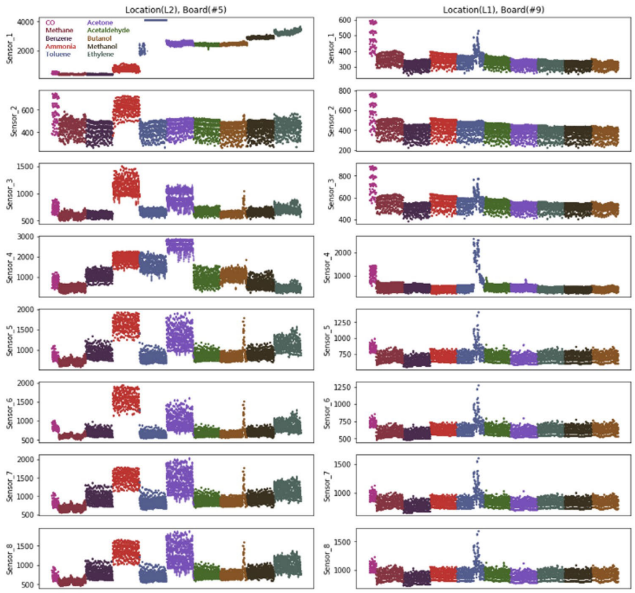

FIGURE 1. The sensor value in the 0–10 second sections of the no. 5 Board at the L2 position and the no. 9 Board at the L1 position.

This paper analyzes the characteristics of not only the temporal information reference dataset but also the spatial information reference dataset. In the temporal information reference dataset, each sensor was observed to be affected by drift and whatever variation arose for each space in the wind tunnel. For this, the data in the 0–10 second section were sampled and the positions where the most and least drift occurred were analyzed for each position and board.

Figure 2 shows the TSNE results for each gas on nine boards at the L2 position. According to the results, the no.

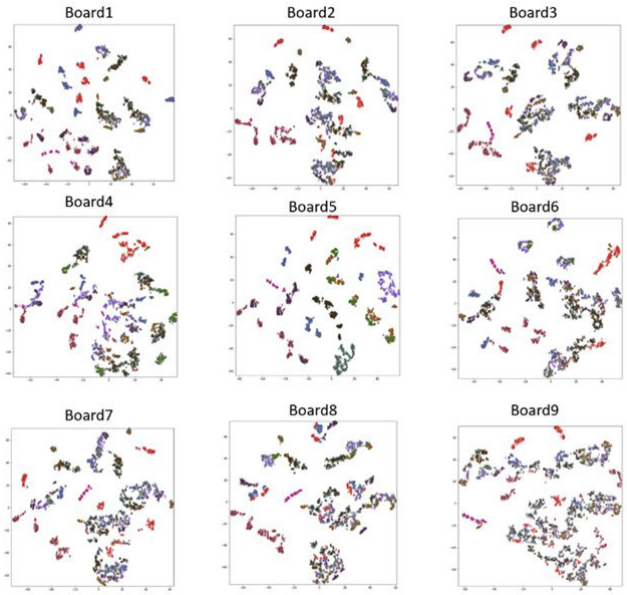

FIGURE 2. TSNE results for each gas on nine boards at the L2 position.

5 Board was strongly affected by the drift effect because it was positioned nearest to the gas exhaust point, so the cluster is formed even before any gas was released. In contrast, clusters rarely formulated for the no. 9 Board positioned farthest from the gas exhaust point; it could be presumed that it was the least influenced by drift.

IV. DRIFT EFFECT ANALYSIS

A. DRIFT EFFECT ANALYSIS METHOD

Before analyzing the data, we converted the sensor voltage value given in the data set to the resistance value resistance values, according to the equation (1)

$$R_{value} = 10k\Omega \times \frac{3.11V - V_{value}}{V_{value}} \tag{1}$$

In general, the instability or drift of the sensor characteristics means the change of the sensitivity or output level due to time, temperature or certain cause. This paper uses zero-offset method to compensate drift, and analyzes the gas data. Assuming that the first 100ms of sensor data is the initial output value of the sensor, and calculate the average value of the 100ms data. This paper uses zero-offset method to compensate drift, and analyzes the gas data. Assuming that the first 100ms of sensor data is the initial output value of the sensor, and calculate the average value of the 100ms data. the sensor data was subtracted by the average value. This is a standard procedure for dealing with the drift in sensor data. Zero-offset subtraction method is as follows:

$$x_{comp} = x - AVG_{100ms}, \quad \forall x \tag{2}$$

B. DRIFT EFFECT ANALYSIS THROUGH BY LOCATION

Figure 3 shows the sensor value for classes in each position at the 0–20 second section. Before gas release, researchers normally expect each sensor to have consistent values for all classes at any position. According to Figure 1, sensors at

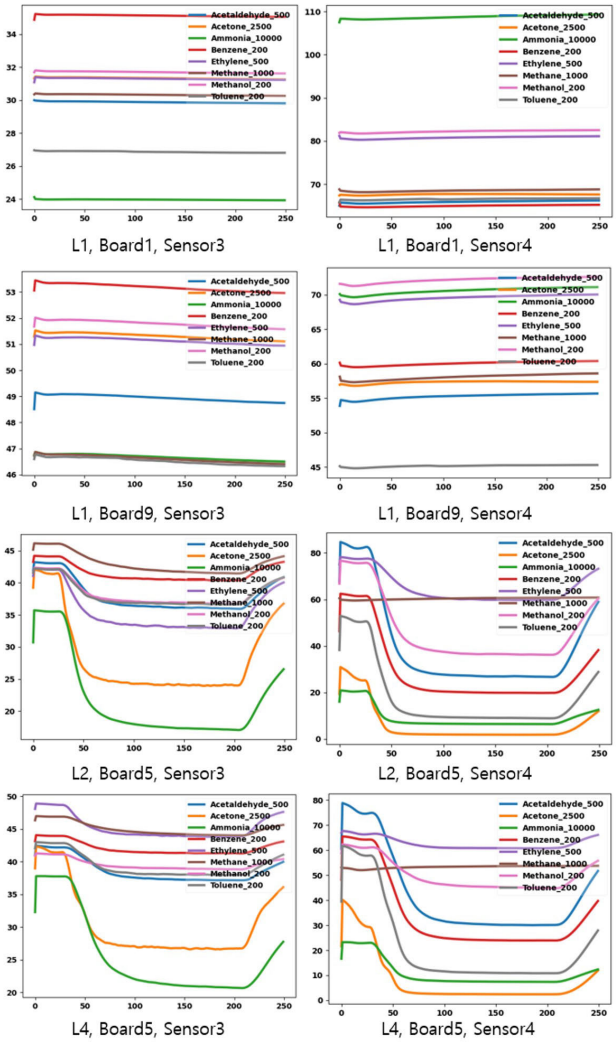

FIGURE 3. Sensor values for every class at specific location.

separate positions had disparate initial values. In addition, the no. 1 and 9 Boards at the L1 position were least influenced by gas as they are located at the ends of the wind tunnel, but their initial values are different. The reason for this is that the sensors on the no. 1 and 9 Boards were affected by drift. Compared to the no. 1 and 9 Boards, which were less affected by gas, sensors' value fluctuations were significant in the two no. 5 Boards that were at the L2 and L4 positions, which were highly influenced by gas.

According to Figure 4, when analyzing changes in the mean and standard deviation, they are more clearly marked when using zero-offset subtraction rather than a raw signal. This shows that while the raw signal has a high value even when there are no changes in the actual sensor value, the zero-offset subtraction method only activates when there is a change in the sensor value.

Figure 5 is a visualization realized by composing all data in the 1–200 second section at each position into a feature vector and performing dimensional reduction by TSNE. In the figure, each class is divided from 0 seconds when using the raw signal. This is attributed to the strong influence of

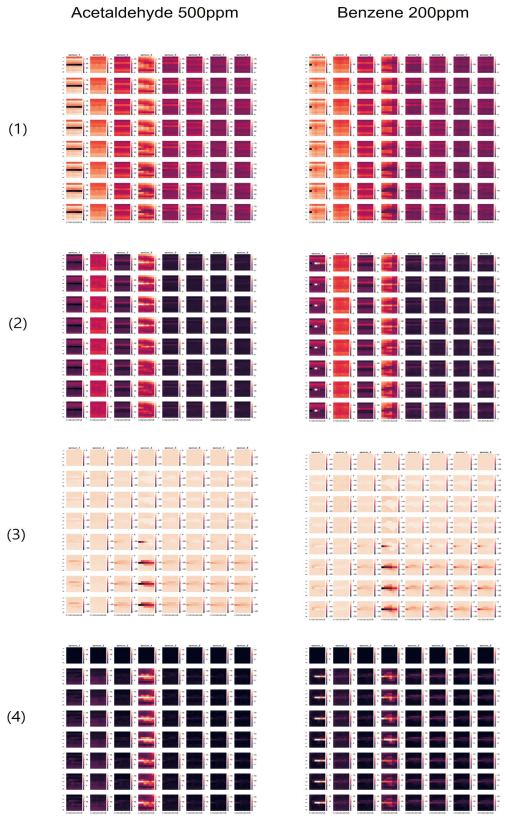

FIGURE 4. Mean and standard deviation of each sensor value at a specific time. (1): Raw signal mean, (2): Raw signal standard deviation, (3): Zero-offset subtracted mean, (4): Zero-offset subtracted standard deviation.

drift. When using the zero-offset subtraction method, gas is identified in each class after gas release, which manifests as a reduced influence of drift.

C. DRIFT EFFECT ANALYSIS THROUGH DEEP NEURAL NETWORK

In general, after gas was released, the 140–200 second section was used to detect gas after a certain amount of time had passed instead of for the entire interval. The model was trained using two methods: raw signal and zero-offset subtraction. As indicated in Figure 6, the date at the 20-second section was utilized. In other words, the one-dimensional time-series data consist of eight gas sensors with N data for 20 seconds (N20x8).

The classes to categorize gas are composed of eight classes (Acetaldehyde_500, Acetone_2500, Ammonia_10000, Benzene_200, Ethylene_500, Methane_1000, Methanol_200, and Toluene_200). The training models are Bidirectional Long Short Term Memory (LSTM) Attention [30] and Bidirectional Temporal Convolution Network (BTCN) [31]. The models for two-dimensional training that include spatial dimensions are CNN [32] and Convolutional Recurrent Neural Network (CRNN) [33]. Softmax, Focal Loss [34], Sphereface [35], Cosface [36], and Arcface [37] functions were employed for Train Loss.

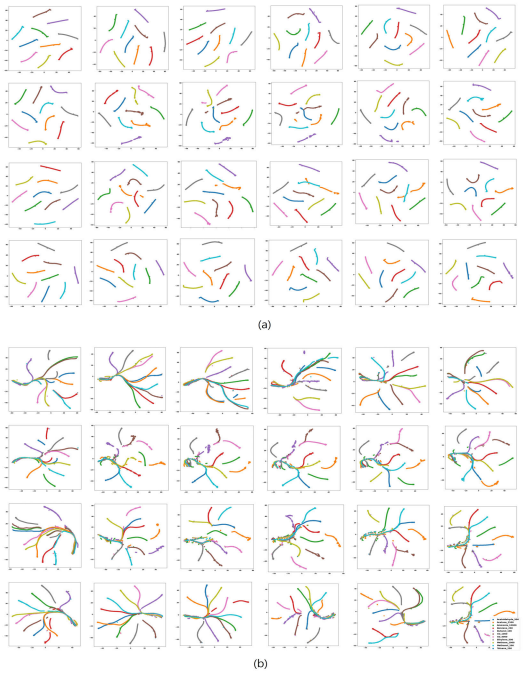

FIGURE 5. Each second of data in a 1–200 second interval visualized by position as a feature vector using the TSNE method.

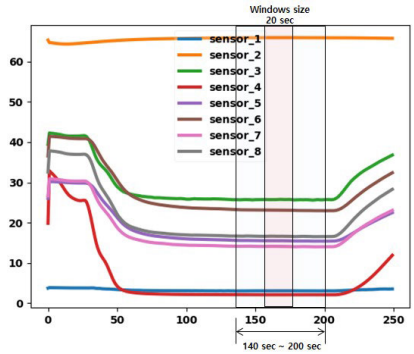

FIGURE 6. 140–200 seconds of data collection with a 20-second window size.

LSTM is the neural network structure designed to enable long- and short-term memory, making up for the disadvantage of existing the RNN that cannot memorize information located far from the output. It is employed for time series processing or natural language processing. RNN applies backpropagation to all time steps from beginning to end, and when a time step is large, it becomes a deep network causing gradient vanishing or exploding problems. To settle this issue, the LSTM cell was suggested that can hold long-term memory. CNN is a neural network model in which learning and testing are available while maintaining the image's space information. While a traditional neural network model comprised only of fully connected layers has the problem of losing space information during the process of flattening the input data, CNN has an advantage in that it improved accuracy by retaining space information through filter calculation. CNN applies sliding convolutional filters across the input data and extracts the feature map.

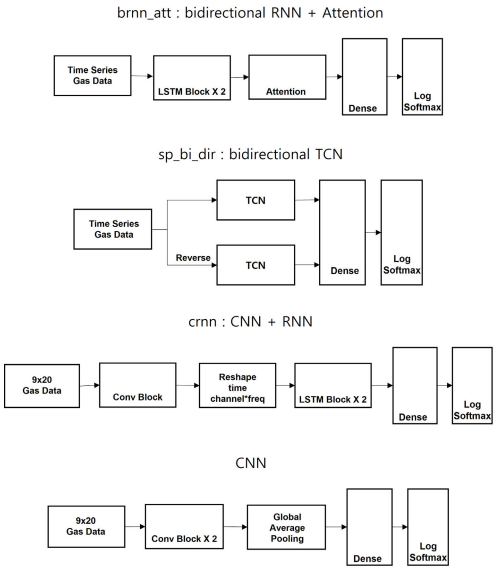

FIGURE 7. Deep learning model using the experiments.

Feature map sizes vary depending on the filter size, stride, padding, and pooling, and users can customize it to their purposes. CRNN is a mixture of CNN and RNN, and it extracts feature sequences by receiving images as inputs and processes classification through RNN based on the extracted feature sequence. It obtains text information through a feature extractor, and converts it into a feature in the form of a sequence with map-to-sequence. Feature sequence holds information related to the image's text, and predicts the text through RNN at the last stage. It has merits as it recognizes sequences from inputs. Temporal Convolution Network (TCN) model uses a 1D-dilated causal convolutional network that expands the receptive field with convolution's locality feature and dilation. It overcomes the limitation of layers, where layers could be accumulated significantly in a simple causal convolution but a larger receptive field cannot be formulated, by applying dilated convolution, so that the receptive field can grow exponentially.

Figure 8 indicates the accuracies of the one-dimensional models at each position.

This paper applies two evaluation indices to assess gas classification models. Accuracy is the ratio of the number of correctly predicted samples to the total number of samples. Loss is an index that represents the error between the answer predicted by the artificial intelligence model and the original answer. For loss functions, the method of applying the Negative Log-Likelihood Loss function (NLL) to results from Log Softmax, Focal Loss that gives more weight to hard-to-detect or misclassified cases, Sphereface that employs Angular margin, Cosface, and Arcface loss function were used.

In the case of using raw signal, the accuracy means at all positions were brnn SoftmaxLoss: 0.59, brnn cosface: 0.53, tcn SoftmaxLoss:0.87, and tcn-cosface: 0.85, while in the case of using zero-offset subtraction, they were brnn SoftmaxLoss: 0.3, brnn cosface: 0.27, tcn SoftmaxLoss:

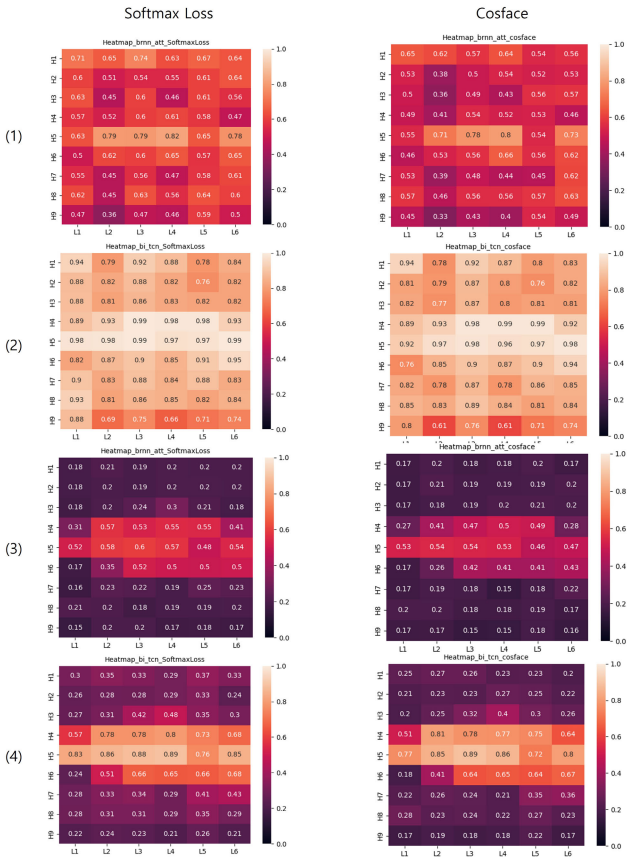

FIGURE 8. Accuracy of the model for one-dimensional data at each location (1) Raw signal brnn, (2) Raw signal tcn, (3) Zero-offset subtracted brnn, (4) Zero-offset subtracted tcn.

0.44, and bi_tcn-cosface: 0.39. According to the experiment's results, the tcn model tends to have higher accuracy than the other models and the models' accuracy tends to be high at positions where the sensor is exposed to gas release. In the case of zero-offset subtraction, the accuracy remarkably declined at the position where the gas did not reach the sensors. Evidently, the accuracy declined when the effect of drift was reduced by removing offset values compared to the raw signal having a biased sensor value even if the actual gas was not released.

The accuracies of the two-dimensional models at each position are as indicated in Figure 9.

When using raw signal, the accuracy means at all positions were cnn SoftmaxLoss: 0.99, cnn cosface: 0.99, crnn-SoftmaxLoss: 0.96, and crnn-cosface: 0.99, while in the case of using zero-offset subtraction, they were cnn SoftmaxLoss: 0.86, cnn-cosface: 0.87, crnn-SoftmaxLoss: 0.66, and crnn-cosface: 0.89. Using raw signals showed higher accuracy than using zero-offset subtraction, and zero-offset subtraction had higher accuracy when using cosface loss. Using two-dimensional data exhibited comparatively higher accuracy because their structure included position information for the nine modules. Additionally, L2, L3, and L4 positions had higher accuracy than the others as they were more exposed to the gas.

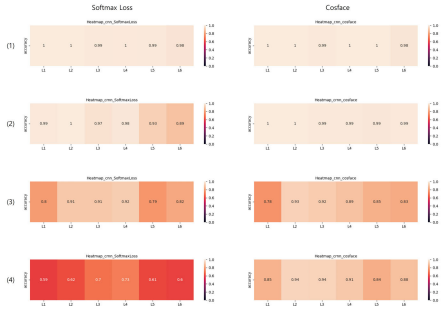

FIGURE 9. Model accuracy with 2D data for each location (1) Raw signal cnn, (2) Raw signal crnn, (3) Zero-offset subtracted cnn, (4) Zero-offset subtracted crnn.

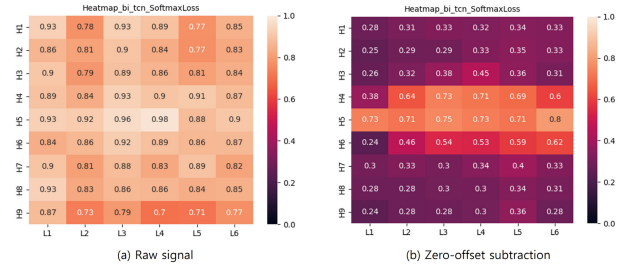

FIGURE 10. Accuracy by location in the range of 0–20 seconds before the gas was released.

Figure 10 describes the accuracy at each position when using the data at the 0–20 second section before gas release. The TCN model and Softmax loss function were employed.

The average accuracy at all positions was 0.86 when using raw signal and 0.42 for the case of zero-offset subtraction. Even without gas release, the model demonstrated higher accuracy since the raw signal was influenced by drift. For zero-offset subtraction, dealing with the drift effect improved but the effect remained at the position heavily exposed to gas, resulting in increased accuracy.

Figure 11 is the result of applying zero-offset subtraction to data at the 0–20 second section that does not have gas exposure. The changes in sensor values for the no. 9 Board at the L1 position are insignificant, –0.8–+0.8, but those at the no. 5 Board at the L2 position are significant, –2–+10. This reveals that changes in sensor value vary depending on the position even in the 0–20 second section has no exposure to gas.

Figure 12 is the result of training the model with three classes—Methanol, Ethylene, and Butanol—that are expected to be least affected by the drift effect at the wind tunnel experiment. The TCN model and SoftMax loss were employed; the average accuracy was 0.79 for the raw signal and 0.57 for zero-offset subtraction. Furthermore, when the data from sensor no. 4, which was the one most affected by drift, were ruled out when using the raw signal, the average accuracy was 0.68; this was 0.51 in the case of zero-offset subtraction.

D. DRIFT EFFECT ANALYSIS THROUGH OUT OF DISTRIBUTION

A typical e-nose system should not classify a particular class until first exposure to gas. Out of Distribution (OOD)

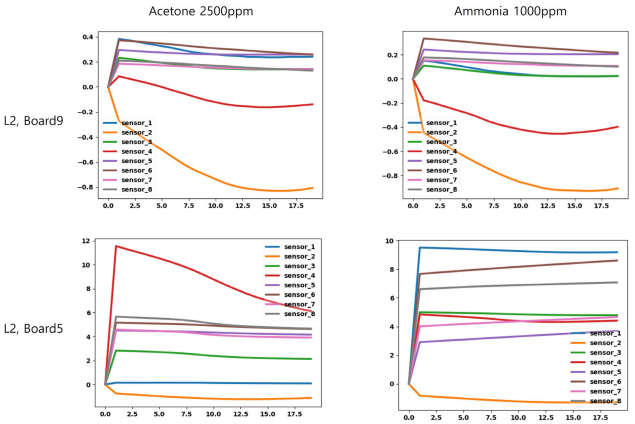

FIGURE 11. Zero-offset subtracted value in the range of 0–20 seconds.

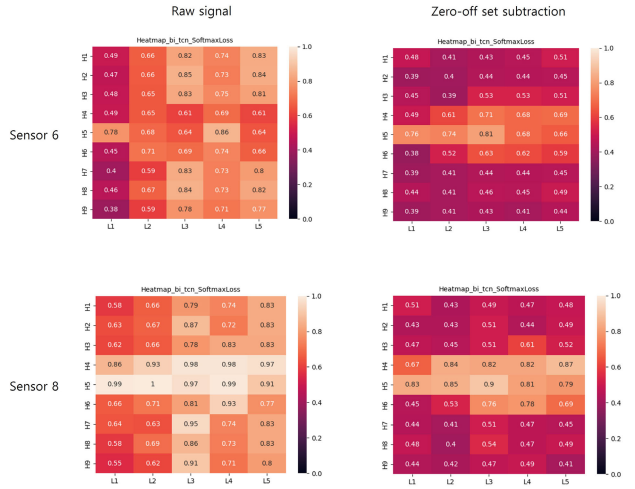

FIGURE 12. The subset least affected by the drift effect using six sensors and eight sensors.

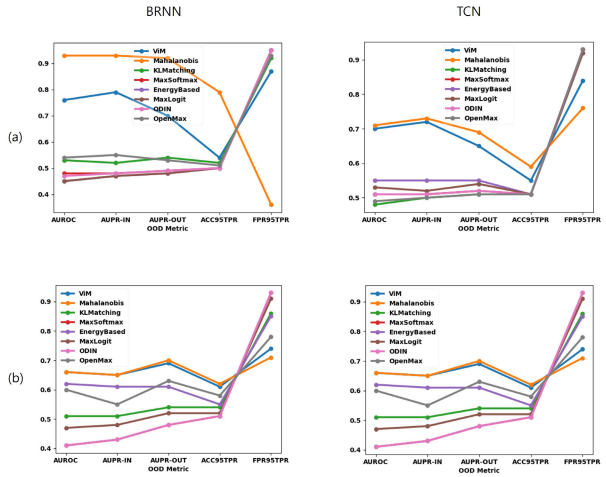

FIGURE 13. When one-dimensional time series data is input, OOD AUROC at any position in 0–20 seconds (a) Raw signal, (b) Zero-offset subtracted.

Detection implements an In-distribution dataset to train a multi-class classification network, and when testing models, its objective is to accurately predict in-distribution test sets while not detecting Out-of-distribution data sets. In most cases, when an Out-of-distribution dataset is input into a

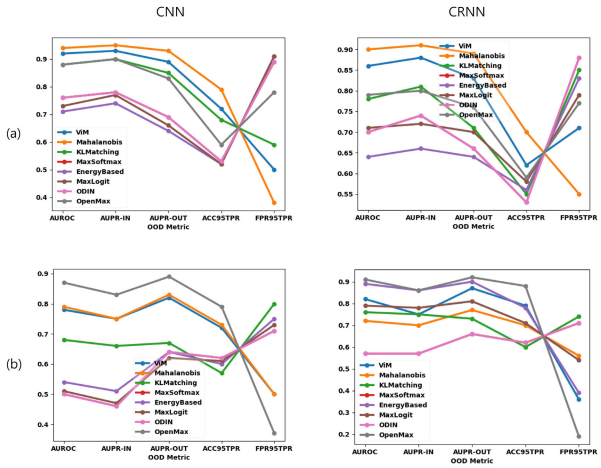

FIGURE 14. When two-dimensional data are input, AUROC of OOD at any position in 0–20 seconds (a) Raw signal, (b) Zero-offset subtracted.

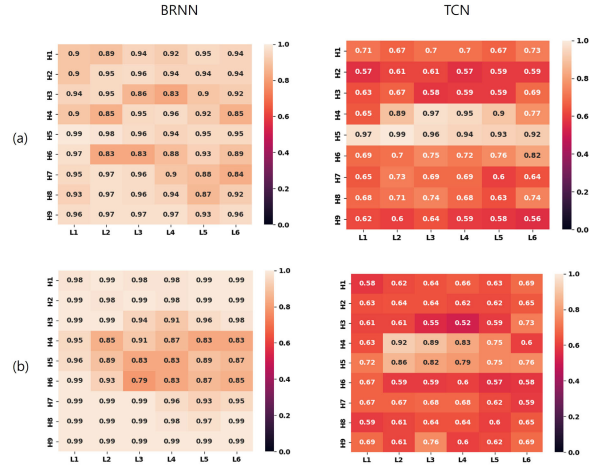

FIGURE 15. AUROC of ODD for each position with 1D input (a) Raw signal, (b) Zero-offset subtracted.

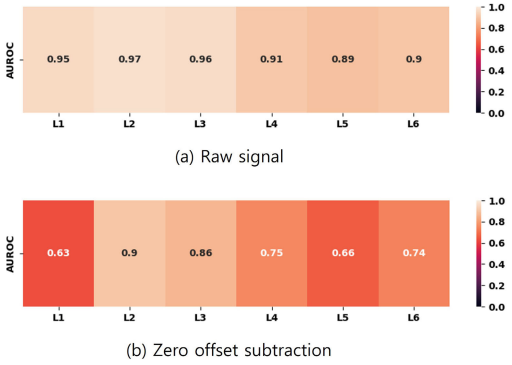

FIGURE 16. AUROC of ODD for each position with 2D input.

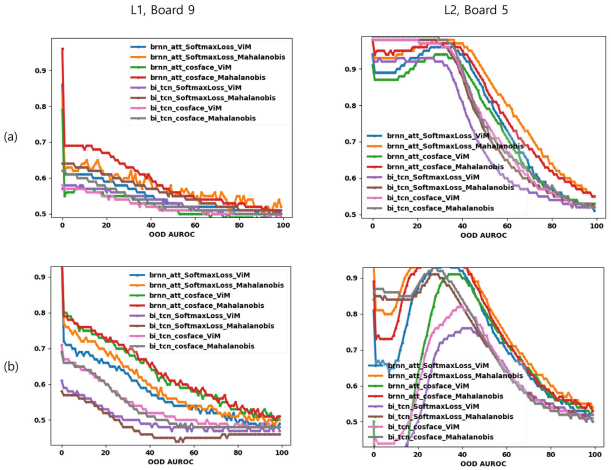

FIGURE 17. AUROC value of ViM and Mahalanobis in OOD for each model, moving a 20-second window within 0–100 seconds in 1-second units (a) Raw signal, (b) Zero-offset subtracted.

model, there are still problems of high-confidence errors being observed. This paper examines the effect of drift on the gas dataset by detecting gas with the OOD method. ViM [38], Mahalanobis [39], KLMatching [40], MaxSoftmax [41], EnergyBased [42], MaxLogit [40], ODIN [43], OpenMax [44] and OOD methods were implemented for the experiment. AUROC was estimated from data of all positions in the 0–20 second gas leak-free section to analyze the drift effect using the OOD method.

According to the results in Figure 13, when using a typical detection model, the accuracy of Softmax was highest, but when using the OOD method, the results that used cosfass loss manifested higher accuracy. Mahalanobis and ViM demonstrated the highest accuracy, and high accuracy was observed when using the raw signal (brnn: 0.93, tcn: 0.71) and when using zero-offset subtraction (brnn: 0.94, tcn: 0.66).

Figure 14 illustrates the results of inputting two-dimensional data that include location information to models. ODD with two-dimensional data input demonstrated the highest accuracy when using Softmax loss, and then Vim, Mahalanobis, and OpenMax showed the highest accuracy in that order.

Figure 15 describes the AUROC results at each position. The gas detection accuracy of the tcn model is high on average for all positions, and in the case of OOD, brnn shows better performance than tcn. However, it is observed that the accuracy of tcn is higher than that of brnn at positions where gas is released.

Figure 16 illustrates the AUROC results at each position when inputting two-dimensional data that includes spatial information. When using the raw signal, the accuracy of Mahalanobis was highest at 0.94, while the accuracy of OpenMax was highest at 0.91 when using zero-offset subtraction.

Figure 17 describes the OOD results of each model in accordance with the time sequence. In the case of the no. 9 Board at the L1 position, it had a high value at the initial stage, which stiffly decreased as time passed. This demonstrates that there were changes in value at the initial stage before gas release. For the no. 5 Board at the L2 position, the increase of AUROC value since the gas release can be noted; the value fluctuates after gas release and the fluctuation decreases as the gas dissipates.

V. CONCLUSION

This paper conducted various experiments related to the drift effect using data sets from a MOx gas sensor array in a wind tunnel Vergara et al. [5]. Since MOx sensors are susceptible to sensor drift, we analyzed the effects of sensor drift on the gas sensor data set from temporal and spatial perspectives. In addition, one-dimensional time series data in the range 140–200 seconds were extracted after the gas was fully released and a variety of deep-learning models were learned based on this input. The training data were raw signal data or data with the zero-offset subtraction method. The experiments of each location were conducted to verify the accuracy of gas classification at different locations, and the location affected by gas release and the location less affected by gas release were analyzed. The results showed that the performance of the TCN model was higher, and We confirmed that the sensor close to the location where the gas is emitted had high accuracy. Also, for the zero offset subtracted data, the accuracy was significantly decreased. This is because the farther sensor from the gas emission location was already outputting a certain level of sensor value before the gas was emitted, and by removing the initial offset value it was confirmed that the actual accuracy is low. Furthermore, to examine the effect of drift on the gas dataset this paper analyzed the drift effect at each location in terms of OOD by calculating the AUROC of OOD at one-second intervals. According to the experimental results, brnn showed high performance with an average AUROC of 0.94 for every location, and also performed well at locations far from where gas was emitted. On the contrary, TCN had a low overall average AUROC of 0.66, but showed relatively high performance for OOD at locations where gas was emitted. This means that even though the overall average of BRNN was higher, in terms of OOD, TCN was superior to BRNN.

Other papers acknowledged that the accuracy of classification from those datasets is exceptionally high compared to other datasets, and reported the problem of datasets unveiled in the previously published paper and the resulting drift effect for the first time. This paper expands the previous paper, by analyzing the drift effect with low signal, zero-offset subtracted signal's mean, and standard deviation value by location and time, and examining it with TSNE, a dimensional reduction method. The Zero-offset subtraction method compensated for the gas data by subtracting the average value of the initial 100ms data acquired from the sensor from the total data. It mitigated the drift effect by deducting the sensor value affected by the drift from the total data, assuming all sensor data were influenced by the drift effect before the initial gas leak. In addition, the accuracy by time and location was analyzed by applying it to various Deep Learning methods. According to the results, we confirmed that gas information is already classified before the gas leaks in terms of temporal and spatial domain. Therefore, the classification accuracy overestimates the actual accuracy that can be obtained due to the drift effect. Based on the results of this study, it is necessary to thoroughly verify the temporal and spatial validity of the gas dataset when using the publicly available gas dataset to develop gas detection algorithms.

ACKNOWLEDGMENT

(Il-Sik Chang, Sung-Woo Byun, Tae-Beom Lim, and Goo-Man Park contributed equally to this work.)

REFERENCES

[1] J. R. Stetter, P. C. Jurs, and S. L. Rose, "Detection of hazardous gases and vapors: Pattern recognition analysis of data from an electrochemical sensor array," *Anal. Chem.*, vol. 58, no. 4, pp. 860–866, Apr. 1986.

[2] K. Persaud and G. Dodd, "Analysis of discrimination mechanisms in the mammalian olfactory system using a model nose," *Nature*, vol. 299, no. 5881, pp. 352–355, Sep. 1982.

[3] J. W. Gardner and P. N. Bartlett, "A brief history of electronic noses," *Sens. Actuators B, Chem.*, vol. 18, nos. 1–3, pp. 210–211, 1994.

[4] A. Ziyatdinov, S. Marco, A. Chaudry, K. Persaud, P. Caminal, and A. Perera, "Drift compensation of gas sensor array data by common principal component analysis," *Sens. Actuators B, Chem.*, vol. 146, no. 2, pp. 460–465, 2010.

[5] A. Vergara, J. Fonollosa, J. Mahiques, M. Trincavelli, N. Rulkov, and R. Huerta, "On the performance of gas sensor arrays in open sampling systems using inhibitory support vector machines," *Sens. Actuators B, Chem.*, vol. 185, pp. 462–477, Aug. 2013.

[6] N. Dennler, S. Rastogi, J. Fonollosa, A. van Schaik, and M. Schmuker, "Drift in a popular metal oxide sensor dataset reveals limitations for gas classification benchmarks," *Sens. Actuators B, Chem.*, vol. 361, Jun. 2022, Art. no. 131668.

[7] A. Vergara, S. Vembu, T. Ayhan, M. A. Ryan, M. L. Homer, and R. Huerta, "Chemical gas sensor drift compensation using classifier ensembles," *Sens. Actuators B, Chem.*, vols. 166–167, pp. 320–329, May 2012.

[8] J. Burgués and S. Marco, "Multivariate estimation of the limit of detection by orthogonal partial least squares in temperature-modulated MOX sensors," *Anal. Chim. Acta*, vol. 1019, pp. 49–64, Aug. 2018.

[9] J. Fonollosa, S. Sheik, R. Huerta, and S. Marco, "Reservoir computing compensates slow response of chemosensor arrays exposed to fast varying gas concentrations in continuous monitoring," *Sens. Actuators B, Chem.*, vol. 215, pp. 618–629, Aug. 2015.

[10] D. Maier, R. Hulasare, B. Qian, and P. Armstrong, "Onitoring carbon dioxide levels for early detection of spoilage and pests in stored grain," *Proc. 9th Int. Work. Conf. Stored Product Protection*, vol. 1, 2006, p. 117.

[11] A. Lilienthal, A. Loutfi, and T. Duckett, "Airborne chemical sensing with mobile robots," *Sensors*, vol. 6, no. 11, pp. 1616–1678, Nov. 2006.

[12] N. Alizadeh, H. Jamalabadi, and F. Tavoli, "Breath acetone sensors as non-invasive health monitoring systems: A review," *IEEE Sensors J.*, vol. 20, no. 1, pp. 5–31, Jan. 2020.

[13] F. Loizeau, H. P. Lang, T. Akiyama, S. Gautsch, P. Vettiger, A. Tonin, G. Yoshikawa, C. Gerber, and N. de Rooij, "Piezoresistive membrane-type surface stress sensor arranged in arrays for cancer diagnosis through breath analysis," in *Proc. IEEE 26th Int. Conf. Micro Electro Mech. Syst. (MEMS)*, Jan. 2013, pp. 621–624.

[14] J. A. Covington, S. Marco, K. C. Persaud, S. S. Schiffman, and H. T. Nagle, "Artificial olfaction in the 21st century," *IEEE Sensors J.*, vol. 21, no. 11, pp. 12969–12990, Jun. 2021.

[15] D. Kwon, G. Jung, W. Shin, Y. Jeong, S. Hong, S. Oh, J.-H. Bae, B.-G. Park, and J.-H. Lee, "Low-power and reliable gas sensing system based on recurrent neural networks," *Sens. Actuators B, Chem.*, vol. 340, Aug. 2021, Art. no. 129258.

[16] S.-Y. Cho, Y. Lee, S. Lee, H. Kang, J. Kim, J. Choi, J. Ryu, H. Joo, H.-T. Jung, and J. Kim, "Finding hidden signals in chemical sensors using deep learning," *Anal. Chem.*, vol. 92, no. 9, pp. 6529–6537, May 2020.

[17] H. Liu, Q. Li, B. Yan, L. Zhang, and Y. Gu, "Bionic electronic nose based on MOS sensors array and machine learning algorithms used for wine properties detection," *Sensors*, vol. 19, no. 1, p. 45, Dec. 2018.

[18] H.-J. Kim and J.-H. Lee, "Highly sensitive and selective gas sensors using p-type oxide semiconductors: Overview," *Sens. Actuators B, Chem.*, vol. 192, pp. 607–627, Mar. 2014.

[19] J.-H. Kim, J. Chun, J. W. Kim, W. J. Choi, and J. M. Baik, "Self-powered, room-temperature electronic nose based on triboelectrification and heterogeneous catalytic reaction," *Adv. Funct. Mater.*, vol. 25, no. 45, pp. 7049–7055, Dec. 2015.

[20] A. T. Güntner, V. Koren, K. Chikkadi, M. Righettoni, and S. E. Pratsinis, "E-nose sensing of low-ppb formaldehyde in gas mixtures at high relative humidity for breath screening of lung cancer?" *ACS Sensors*, vol. 1, no. 5, pp. 528–535, May 2016.
[21] S. Kouda, T. Bendib, S. Barra, and A. Dendouga, "ANN modeling of an industrial gas sensor behavior," in *Proc. Int. Conf. Commun. Electr. Eng. (ICCEE)*, Dec. 2018, pp. 1–4.
[22] G. Jung, H. Kim, Y. Jeong, Y. Hong, M. Wu, S. Hong, W. Shin, D. Jang, and J.-H. Lee, "Accurate identification of gas type and concentration using DNN reflecting the sensing properties of MOSFET-type gas sensor," in *Proc. IEEE Int. Symp. Olfaction Electron. Nose (ISOEN)*, May 2019, pp. 1–4.
[23] J. Chen, L. Wang, S. Duan, and A. Mixed-Kernel, "Variable-dimension memristive CNN for electronic nose recognition," *Neurocomputing*, vol. 461, pp. 129–136, Oct. 2021.
[24] Y. Zou and J. Lv, "Using recurrent neural network to optimize electronic nose system with dimensionality reduction," *Electronics*, vol. 9, no. 12, p. 2205, Dec. 2020.
[25] Z. Jiang, P. Xu, Y. Du, F. Yuan, and K. Song, "Balanced distribution adaptation for metal oxide semiconductor gas sensor array drift compensation," *Sensors*, vol. 21, no. 10, p. 3403, May 2021, doi: 10.3390/s21103403.
[26] Y. Luo, S. Wei, Y. Chai, and X. Sun, "Electronic nose sensor drift compensation based on deep belief network," in *Proc. 35th Chin. Control Conf. (CCC)*, Jul. 2016, pp. 3951–3955.
[27] K. Yan, L. Kou, and D. Zhang, "Learning domain-invariant subspace using domain features and independence maximization," *IEEE Trans. Cybern.*, vol. 48, no. 1, pp. 288–299, Jan. 2018.
[28] B. Liu, X. Zeng, F. Tian, S. Zhang, and L. Zhao, "Domain transfer broad learning system for long-term drift compensation in electronic nose systems," *IEEE Access*, vol. 7, pp. 143947–143959, 2019.
[29] K. Yan and D. Zhang, "Correcting instrumental variation and time-varying drift: A transfer learning approach with autoencoders," *IEEE Trans. Instrum. Meas.*, vol. 65, no. 9, pp. 2012–2022, Sep. 2016.
[30] S. Hochreiter and J. Schmidhuber, "Long short-term memory," *Neural Comput.*, vol. 9, no. 8, pp. 1735–1780, Nov. 1997, doi: 10.1162/neco.1997.9.8.1735.
[31] S. Bai, J. Z. Kolter, and V. Koltun, "An empirical evaluation of generic convolutional and recurrent networks for sequence modeling," 2018, *arXiv:1803.01271*.
[32] A. Krizhevsky, I. Sutskever, and G. E. Hinton, "ImageNet classification with deep convolutional neural networks," *Commun. ACM*, vol. 60, no. 6, pp. 84–90, May 2017, doi: 10.1145/3065386.
[33] B. Shi, X. Bai, and C. Yao, "An end-to-end trainable neural network for image-based sequence recognition and its application to scene text recognition," *IEEE Trans. Pattern Anal. Mach. Intell.*, vol. 39, no. 11, pp. 2298–2304, Nov. 2017, doi: 10.1109/TPAMI.2016.2646371.
[34] T.-Y. Lin, P. Goyal, R. Girshick, K. He, and P. Dollar, "Focal loss for dense object detection," in *Proc. IEEE Int. Conf. Comput. Vis. (ICCV)*, Oct. 2017, pp. 2999–3007, doi: 10.1109/ICCV.2017.324.
[35] W. Liu, Y. Wen, Z. Yu, M. Li, B. Raj, and L. Song, "SphereFace: Deep hypersphere embedding for face recognition," in *Proc. IEEE Conf. Comput. Vis. Pattern Recognit. (CVPR)*, Jul. 2017, pp. 6738–6746, doi: 10.1109/CVPR.2017.713.
[36] H. Wang, Y. Wang, Z. Zhou, X. Ji, D. Gong, J. Zhou, Z. Li, and W. Liu, "CosFace: Large margin cosine loss for deep face recognition," in *Proc. IEEE/CVF Conf. Comput. Vis. Pattern Recognit.*, Jun. 2018, pp. 5265–5274, doi: 10.1109/CVPR.2018.00552.
[37] J. Deng, J. Guo, N. Xue, and S. Zafeiriou, "ArcFace: Additive angular margin loss for deep face recognition," in *Proc. IEEE/CVF Conf. Comput. Vis. Pattern Recognit. (CVPR)*, Jun. 2019, pp. 4685–4694, doi: 10.1109/CVPR.2019.00482.
[38] H. Wang, Z. Li, L. Feng, and W. Zhang, "ViM: Out-of-distribution with virtual-logit matching," in *Proc. IEEE/CVF Conf. Comput. Vis. Pattern Recognit. (CVPR)*, Jun. 2022, pp. 4911–4920, doi: 10.1109/CVPR52688.2022.00487.
[39] K. Lee, K. Lee, H. Lee, and J. Shin, "A simple unified framework for detecting out-of-distribution samples and adversarial attacks," in *Proc. NIPS*, 2018, pp. 7167–7177.
[40] D. Hendrycks, "Scaling out-of-distribution detection for real-world settings," in *Proc. Int. Conf. Mach. Learn.*, 2022, pp. 8259–8773.
[41] D. Hendrycks and K. Gimpel, "A baseline for detecting misclassified and out-of-distribution examples in neural networks," 2016, *arXiv:1610.02136*.
[42] W. Liu, X. Wang, D. J. Owens, and Y. Li, "Energy-based out-of-distribution detection," in *Proc. NIPS 34th Int. Conf. Neural Inf. Process. Syst.*, Dec. 2020, pp. 21464–21475.
[43] S. Liang, Y. Li, and R. Srikant, "Enhancing the reliability of Out-of-distribution image detection in neural networks," 2017, *arXiv:1706.02690*.
[44] A. Bendale and T. E. Boult, "Towards open set deep networks," in *Proc. IEEE Conf. Comput. Vis. Pattern Recognit. (CVPR)*, Jun. 2016, pp. 1563–1572, doi: 10.1109/CVPR.2016.173.

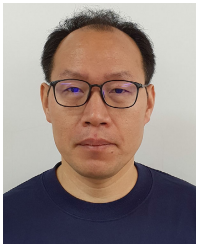

IL-SIK CHANG received the B.S. degree in electronics engineering from Honam University, Gwangju, South Korea, in 2001, and the M.S. degree from Seoul National University of Science and Technology, Seoul, South Korea, in 2011, where he is currently pursuing the Ph.D. degree with the Department of Information Technology and Media Engineering. His main research interests include deep learning, data analysis, and image processing.

SUNG-WOO BYUN received the B.S. and Ph.D. degrees from the Department of Computer Science, Sangmyung University, Seoul, South Korea, in 2014 and 2021, respectively. He is currently a Senior Researcher with Korea Electronics Technology Institute, South Korea. His main research interests include signal processing, artificial intelligence, and personalized media processing.

TAE-BEOM LIM (Member, IEEE) received the B.S. degree in physics and the M.S. degree in computer science from Sogang University, Seoul, South Korea, in 1995 and 1997, respectively, and the Ph.D. degree in information and communication engineering from Konkuk University, Seoul, in 2012. Since 2002, he has been with Korea Electronics Technology Institute, South Korea, where he is currently the Regional President. His research interests include digital twin systems, autonomous vehicle technologies, the intelligent IoT, and UI/UX.

GOO-MAN PARK received the B.S. degree in electronics engineering from Hankuk Aviation University and the M.S. and Ph.D. degrees in electronics engineering from Yonsei University. He was a Senior Engineer with Samsung Electronics, Suwon, South Korea. He is currently a Professor with the Department of Electronics and IT Media Engineering, Seoul National University of Science and Technology, Seoul, South Korea. His current research interests include computer vision and immersive media.